

# A Convenient Approach to Synthesize Stable Silver Nanoparticles and Silver/Polystyrene Nanocomposite Particles

Desong Wang, Jing An, Qingzhi Luo, Xueyan Li, Minna Li

College of Sciences, Hebei University of Science and Technology, Hebei, Shijiazhuang 050018, China

Received 25 October 2007; accepted 29 February 2008

DOI 10.1002/app.28442

Published online 8 September 2008 in Wiley InterScience (www.interscience.wiley.com).

**ABSTRACT:** In this study, silver nanoparticles were prepared by the reduction of silver nitrate in SDS+ isopentanol/styrene/H<sub>2</sub>O reverse microemulsion system using sodium citrate as reducing agent. The Ag/PS nanocomposite particles were prepared by *in situ* emulsion polymerization of the styrene system containing silver nanoparticles that did not separate from the reaction solution. The polymerization dynamic characteristic was studied, at the same time, silver nanoparticles and the encapsulation of composite particles were characterized by Fourier-transform-infrared spectroscopy (FTIR), transmission electron microscopy (TEM), X-ray diffraction (XRD) measurement, UV–vis diffuse reflectance spectroscopy, and X-ray photoelectron

spectroscopy (XPS). The results of TEM and UV–vis absorption spectra showed that well-dispersed silver nanoparticles have a narrow size distribution. XRD showed that Ag and Ag/PS nanocomposite particles were less than 10 and 20 nm in size, which is similar to those observed by TEM. The results of XPS spectra revealed that the microemulsion system can stabilize the silver nanoparticles from aggregation and provided supporting evidence for the polystyrene encapsulated silver nanoparticle structure. © 2008 Wiley Periodicals, Inc. *J Appl Polym Sci* 110: 3038–3046, 2008

**Key words:** silver nanoparticles; nanocomposite particles; microemulsion; emulsion polymerization

## INTRODUCTION

Metal nanoparticles show peculiar optical, magnetic, and electronic properties that bulk solid or isolated molecules do not usually exhibit.<sup>1–3</sup> Recently, there has been immense interest in the fabrication of composite materials consisted of polymer-encapsulated particles. It is now well-established that the polymers are excellent host materials for nanoparticles of metals and semiconductors.<sup>4–11</sup> When the nanoparticles are embedded or encapsulated in polymer, the polymer acts as surface capping agent, the particle size is controlled well within the desired regime and casting of film becomes easier.<sup>12,13</sup> The technique of polymer encapsulation is becoming more and more popular since polymer-encapsulated particles offer very interesting actual and potential applications. Most methods of encapsulation including emulsion polymerization, surfactant-free emulsion polymerization, emulsion-like polymerization, suspension polymerization, and dispersion polymerization have been employed.

Among all the metal/polymer composites, silver composites are found important applications

in material technologies like optical materials,<sup>14</sup> catalytic systems, antibacterial materials,<sup>15,16</sup> chemical nanosensors, and surface-enhanced Raman scattering (SERS).<sup>17</sup> However, the big challenge encountered in preparing silver/polymer nanoparticle encapsulation is that the nanoparticles cannot be dispersed in polymer matrix at the nanolevel by conventional techniques, because the surface energy of tiny silver particles is very high, and these particles tend to agglomerate during mixing. For application in optoelectronics and electronics, the control of particle size and their uniform distribution within the polymer is the key technology based on the nanoparticles in polymers. Improved stability of silver nanoparticles has been understood in polystyrene (PS)<sup>18,19</sup> possibly because of the presence of free electrons in functional groups of the polymer chains, which allow the particles to be held more firmly by the functional groups. In recent literatures, several processes have been described to synthesize particles that consist of an silver core surrounded by polystyrene shell.<sup>20–22</sup> Zhang et al. have described the dispersion polymerization of styrene in a water–ethanol (1/6 w/w) medium, with poly(*N*-vinyl pyrrolidone) (PVP) as stabilizer and 2,2V-azobisisobutyronitrile (AIBN) as initiator in the presence of silver nanoparticles through ultrasonic irradiation inducement.<sup>23</sup> The inorganic nanoparticles in the aqueous solution can redisperse more

Correspondence to: D. Wang (dswang06@126.com.cn).  
Contract grant sponsor: Hebei Nature Science Council.

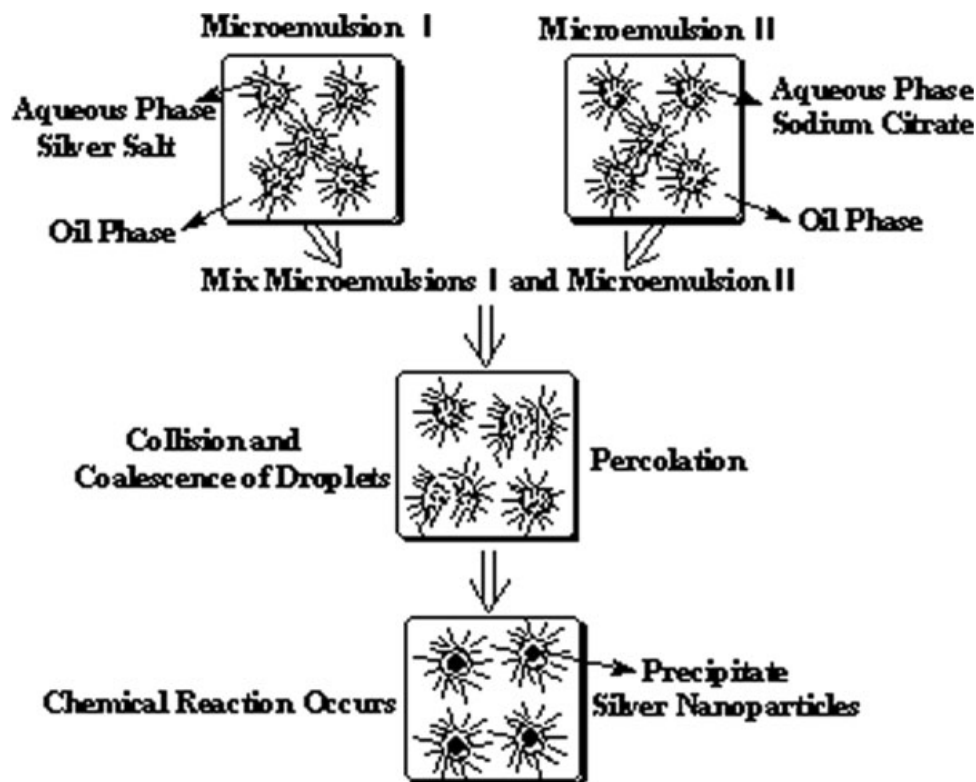


Figure 1 Proposed mechanism for the formation of metal particles by microemulsion approach.

effectively through ultrasonic irradiation than by conventional stirring. To our knowledge, there is no description in the literatures of synthesizing and dispersing silver nanoparticles in microemulsion with styrene as oil phase and preparation of silver/polystyrene nanocomposite particles by using *in situ* emulsion polymerization of the styrene system in the presence of silver nanoparticles.

In this article, we report a simple and novel method to synthesize silver nanoparticles in water-in-oil microemulsion using silver nitrate solubilized in the water core of one microemulsion as source of silver ions, sodium citrate solubilized in the water core of another microemulsion as reducing agent, styrene as the oil phase, sodium dodecyl sulfate (SDS) as the emulsifier, and isopentanol as the coemulsifier. The styrene system described earlier is directly dispersed into water to form the ordinary emulsion and then polymerized to fabricate the silver/polystyrene nanocomposite particles. As a result, the Ag nanoparticles could be surrounded by polystyrene and dispersed evenly into the polystyrene matrix in nanosizes. The polymer composites prepared by the earlier method could possess some performances different from those of the ordinary polymer composites, and therefore, it may be a very interesting and promising approach to fabricate silver and other polymer nanocomposites by this method.

## EXPERIMENTAL

### Materials

All the reagents used were of AR grade. Double distilled water was used throughout the experiment. Silver nitrate and sodium citrate used in this study were purchased from Beijing Chemical Reagent Factory. The styrene monomer was supplied by Beijing Fuxing Chemical Reagent Factory (Beijing, China), and it was washed three times with 10% aqueous solution of sodium hydroxide and distilled water, respectively, to remove the inhibitors, dried with anhydrous sodium sulfate, and then vacuum distilled. The sealed purified styrene was stored at 4°C until required. Sodium dodecyl sulfate (SDS) and isopentanol were used as surfactant and assistant surfactant, respectively, potassium persulfate (KPS) was used as initiator for emulsion polymerization of styrene. PVP K-30 can prevent Ag nanoparticles from aggregation in the reaction.

### Synthesis of silver in styrene microemulsion

Ag nanoparticles were prepared in reverse microemulsion with styrene as oil phase. A schematic picture of this process is represented in Figure 1. First, the microemulsions I and II were prepared by mixing the same volume (1.5 mL) of aqueous solution of

AgNO<sub>3</sub> (0.2M) and sodium citrate (0.4M) into 0.86M and 1M SDS/styrene solution, respectively. The overall concentrations of AgNO<sub>3</sub> and sodium citrate were  $8.8 \times 10^{-5}M$  and  $2 \times 10^{-4}M$ , respectively. The molar ratio of sodium citrate and AgNO<sub>3</sub> was held constant at a value of 2. Second, the microemulsion containing sodium citrate was added dropwise into another microemulsion under continuous stirring in the constant temperature magnetism stirrer at 30°C for 2 h, and then the microemulsion containing Ag nanoparticles was formed. The silver colloid can be used directly as monomer to synthesize Ag/PS composite particles.

### Synthesis of silver/polystyrene nanocomposite particles

The Ag/PS composite particles were prepared according to the following steps. First, 30 mL of silver colloid solution was dispersed into 160 mL deionized and distilled water with ultrasonic vibrations for 30 min to obtain a uniform suspension. Second, 1 g of PVP used as stabilizer were added into this mixture under continuous stirring in the constant temperature magnetism stirrer. After bubbling nitrogen through the reaction medium for 30 min, the mixed reaction system was introduced into a 250-mL three-necked flask and 0.1 g of KPS (initiator) was added to the emulsion polymerization solution when temperature is invariable at 70°C, cooling water was circulated to decrease reaction system temperature, and constant N<sub>2</sub> purging rate was maintained. Fourth, the polymerized composite particles were deposited by sodium chloride and washed several times with deionized water, after that dipped into ethanol for 5 h. Finally, the composite particles were dried at 60°C in a vacuum box for 48 h. These particles are now used for characterization and spectroscopic applications.

### Characterization experiments

Morphology of as-synthesized silver colloids and composite particles was characterized by transmission electron microscopy (TEM), which was a tecnai G2 F20 electron microscopy instrument, equipped with an energy dispersive X-ray (EDX) detector. The samples of TEM were prepared by dispersing the final nanoparticles in ethanol; the dispersion was then dropped on carbon-copper grids. Size distribution and number-average particle diameters were obtained using the Image Pro Plus Image Analysis System. Fourier transform infrared spectra (FTIR) of the samples were recorded on spectrometer (SHIMADZA) in the range of 400–4000 cm<sup>-1</sup>. Measurements were performed in the transmission mode in spectroscopic grade KBr pellets for all the powders.

The composites X-ray diffraction (XRD) patterns were performed in the range of  $2\theta = 10^\circ\text{--}90^\circ$  on a Rigaku D/MAX-2500 diffractometer, using Cu K $\alpha$  radiation ( $\lambda = 0.15406$  nm) as X-ray source, operated at 40 kV and 100 mA. Crystallite size of Ag nanoparticle and Ag/PS composite particle can be calculated from the line broadening by Scherrer's formula. A Varian Cary 100 Scan UV-visible system equipped with an integrating sphere attachment was used to obtain the reflectance spectra of the catalysts over a range of 200–800 nm. Integrating sphere USRS-99-010 was employed as a reflectance standard. XPS measurements were performed in a Perkin-Elmer PHI1600 ESCA system with an Mg K $\alpha$  X-ray source. All binding energies were referenced to the C 1s peak at 284.9 eV of the surface adventitious carbon.

## RESULTS AND DISCUSSION

### Polymerization dynamic characteristic

The conversion curve was recorded with a dilatometer. The monomer conversion and polymerization rate as functions of reaction time are obtained by the rate of volume shrinkage. In Figure 2, Curve I has the same shape with Curve II, and so does Curve III with Curve IV. It indicates that the emulsion polymerization of styrene in the presence of Ag nanoparticles is similar to the dynamic formula of emulsion polymerization. The result of Curve I higher than Curve II shows that the emulsion polymerization in the presence of Ag nanoparticles has higher monomer conversion, and that the polymerization conversion can reach about 90% in 3.0 h, and the polymerization rate can reach the maximum in 26 min. The polymerization in the presence of Ag nanoparticles was inhomogeneous system at the outset of the reaction, and Ag nanoparticles can become the nucleation centers. So the polymerization of styrene in the presence of Ag nanoparticles is similar to seed emulsion polymerization. Much more lattices were formed with the nucleus effect of Ag nanoparticles in the whole process. As a result, the monomer conversion and the rate of emulsion polymerization are higher than those of typical emulsion polymerization.

### Particle size and morphology

The TEM micrographs and particle size distribution histogram of Ag and Ag/PS composite particles are clearly displayed in Figure 3. As seen in Figure 3(a1), the particles exhibit a regular spherical shape homogeneously distributed. In Figure 3(a2), the size distribution of silver nanoparticles is narrow and the average diameter of the Ag nanoparticles is  $\sim 5.9$  nm. In Figure 3(b), the average diameter of Ag/PS

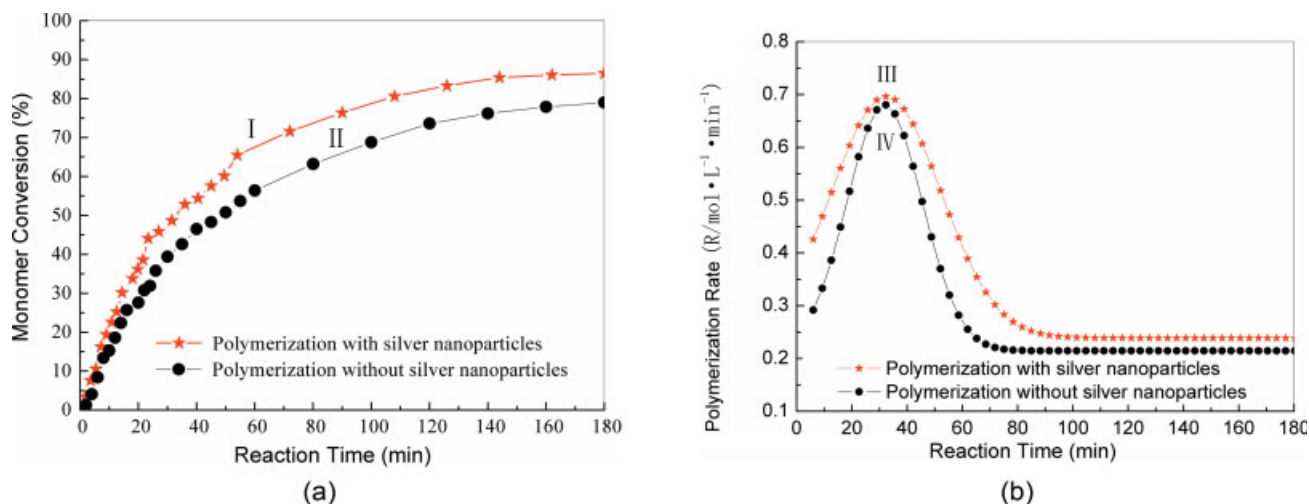


**Figure 2** Monomer conversion and polymerization rate as functions of reaction time. [Color figure can be viewed in the online issue, which is available at [www.interscience.wiley.com](http://www.interscience.wiley.com).]

composite particles are monodispersed about 12.6 nm and the surface of the polystyrene particles obtained in the presence of Ag nanoparticles is smooth and no silver bead is detected on the whole surface of the samples. These observations can lead to the conclusion that the Ag nanoparticles are encapsulated in the polystyrene particles in the course of the emulsion polymerization process and the thickness of polystyrene layer is about 2–6 nm. We could make it clear that the surface of Ag nanoparticles was modified by the surfactant SDS when silver was synthesized in microemulsion, so Ag nanoparticles dispersed well without aggregations that caused by the high surface energy. We found that the polystyrene particles obtained by emulsion polymerization are rather small (no more than 20 nm) and monodisperse. It is because that the large amounts of surfactant (as much as 30–35%) added to the system when synthesize silver in styrene microemulsion and it is much more than the ordinarily dose of emulsion polymerization.

### FTIR analysis

Figure 4 shows the IR spectra of Ag, pure PS, and Ag/PS composite. As shown in Figure 4, the characteristic peaks of PS (3012, 2885, 1413, 1400, 690  $\text{cm}^{-1}$ ) and Ag nanoparticle (3400, 3140, 1600, 1364, 1000  $\text{cm}^{-1}$ ) could be found in the spectrum of Ag/PS composite particles. Comparing the FTIR absorption spectra of PS and Ag/PS composite, the main characteristic peaks of Ag/PS are assigned as followed<sup>23</sup>: =C–H stretching mode for the benzenoid rings occur at 3010  $\text{cm}^{-1}$ , the peak at 2885  $\text{cm}^{-1}$  is attributed to the saturation band C–H stretching mode, the weak peak from 2000 to 1600  $\text{cm}^{-1}$  is attributed to C–H bending mode for benzenoid rings, the

peak at 1600, 1413, and 1450  $\text{cm}^{-1}$  is attributed to the benzenoid rings framework stretching vibration mode, the peak at 755 and 698  $\text{cm}^{-1}$  are attributed to C–H bending vibration mode for single substituent benzene. C=O and C–N stretching mode for PVP occur at 1677  $\text{cm}^{-1}$  and 1364, respectively. Compared with criterion FTIR spectra, the C=O stretching mode for PVP transferred from 1664 to 1677. The results showed that PVP is the transition layer between Ag nanoparticle and polystyrene particle, the N and O atoms in PVP had formed chemical bond with silver atoms on the surfaces of Ag nanoparticles in the Ag/PS composite particles, which had influenced the coupling effect between C=O and C–N.

### X-ray diffraction studies

Figure 5 shows a typical X-ray diffraction (XRD) patterns of the sample of Ag synthesized in microemulsion, PS and Ag/PS composite particles obtained through emulsion polymerization, respectively. In Figure 5, the major three strong characteristic peaks of Ag and Ag/PS composite particles lied in  $2\theta = 38.157^\circ$ ,  $44.352^\circ$ , and  $64.516^\circ$ , which are corresponding with crystal face of (111), (200), and (220) of Ag nanoparticle.<sup>24</sup> It is also easily found that the characteristic peak of PS ( $2\theta = 13.653^\circ$ ) occurs in Ag/PS composite particles. All the reflection peaks can be indexed to face-centered cubic silver and the results provide supporting evidence for the polystyrene encapsulated Ag nanoparticle structure. Moreover, this indicates that Ag/PS composite particles prepared by emulsion polymerization did not change the crystalline structure of neat Ag. The mean size of silver nanoparticle and Ag/PS composite particle were 6.7 and 16.8 nm respectively, calculated using



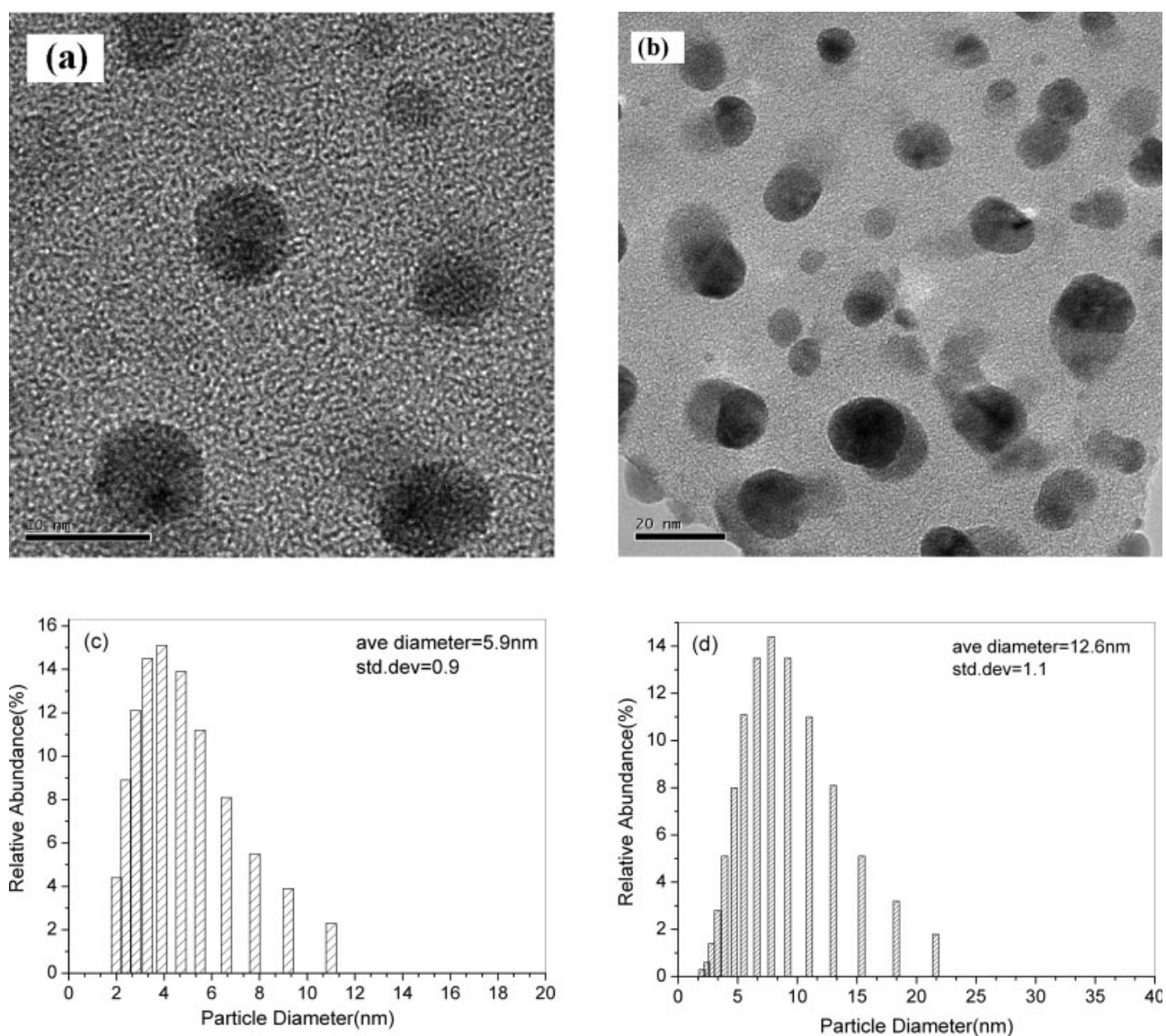


**Figure 3** TEM micrograph and size distribution of Ag and Ag/PS nanoparticles: (a) TEM of Ag, (b) TEM of Ag/PS, (c) size distribution of Ag, and (d) size distribution of Ag/PS.

Scherrer's formula. The results are in accordance with the results of TEM.

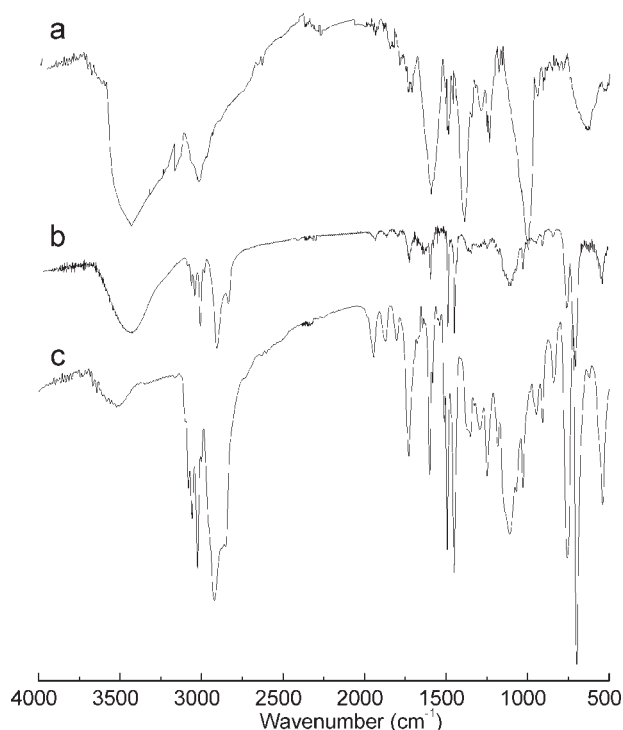
#### UV-vis diffuse reflectance spectra

Figure 6 shows the UV-vis absorption spectrum of Ag nanoparticles and Ag/PS composite particles. From Figure 6, the strong absorption peak at  $\sim 392$  nm of Ag synthesized in microemulsion corresponded well with that of pure Ag nanoparticles,<sup>25,26</sup> and the good symmetric absorption peak implies that the size distribution of the Ag nanoparticles is narrow.<sup>27</sup> From Curve (c) in Figure 6, it can be found that the maximum absorption gives rise to a red shift from 392 to 411 nm when the Ag nanoparticles added into polystyrene by emulsion polymerization to prepare Ag/PS composite particles. It

means that the size of Ag nanoparticle in nanocomposites increased and a few silver aggregates formed in polymerization.

#### XPS analysis

To gain more information on encapsulation state of the obtained Ag nanoparticles, X-ray photoelectron spectroscopy (XPS) technique was employed to detect the composition of the product. Figure 7 shows survey X-ray photoelectron spectra of the sample of Ag/PS composite particles obtained through emulsion polymerization. In the spectra, the atoms of C, O, S, N can be detected. The occurrence of carbon and nitrogen signals confirmed the presence of PVP on the surface of the Ag nanoparticles. XPS spectrum of C1s [Fig. 7(b)], O1s [Fig. 7(c)], and



**Figure 4** FTIR spectra of particles: (a) Ag, (b) Ag/PS composite, and (c) PS.

N1s [Fig. 7(d)] have been fitted by multiple Gaussians. Through curve fitting three peaks were observed at binding energy of 284.9, 286.3, 288.6 eV for C1s and two peaks at 532.0, 533.4 eV for O1s. The binding energies of the two peaks (284.9 and 286.3) can be assigned to C–C and C–N carbon atoms in the PVP, respectively. The signal of C1s 288.6 eV and O1s at 532.0 eV, respectively, can be assigned to the bonds of C=O and Ag–O in the composites, which confirms that the PVP led to tight combine between Ag and PS. Curve in the N1s region [Fig. 7(d)] shows a peak at 402.7 eV. Comparing with pure PVP, the N1s peak shifts to a higher

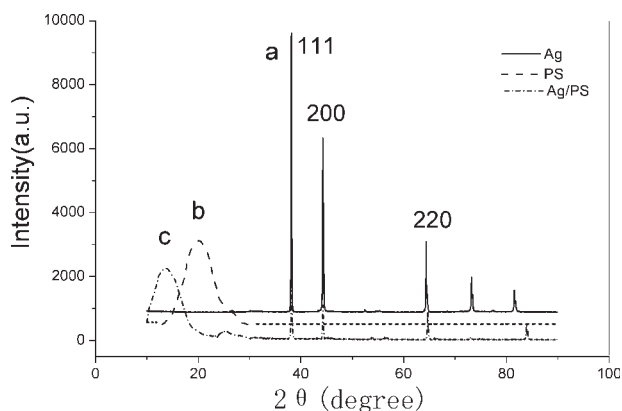


**Figure 5** X-ray diffraction patterns of particles: (a) Ag, (b) PS, and (c) Ag/PS particles.

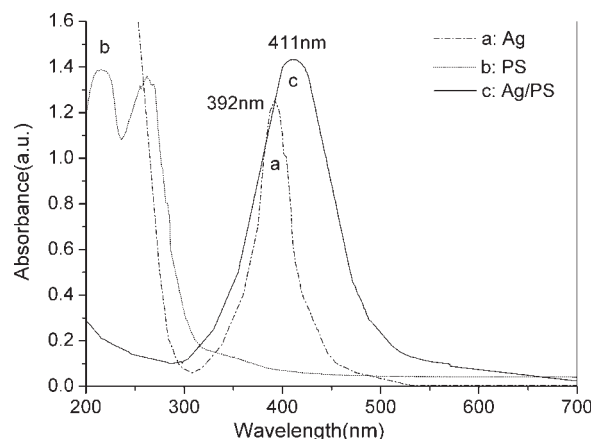


**Figure 6** UV-vis diffuse reflectance spectra of nanoparticles: (a) Ag, (b) PS, and (c) Ag/PS particles.

binding energy and it implied that the decrease of electron density probably due to both interaction between PVP molecule and the Ag nanoparticle core. Curve in the S1s region [Fig. 7(a)] shows a peak at 168.5 eV. The occurrence of sulfur signal confirmed the presence of SDS on the surface of the Ag nanoparticles. The content of Ag particles in the surface of Ag/PS composite particles was so little that the peak of binding energy of Ag element disappeared in Figure 7(a). The results also provided supporting evidence for the polystyrene encapsulated Ag nanoparticle structure.

#### The formation mechanism of Ag/PS nanocomposite particles

Ag/PS composite particles were prepared by a convenient method as shown in Figure 8. This approach has two essential features: (1) the synthesis of Ag nanoparticles by reducing  $\text{AgNO}_3$  by sodium citrate via inversed microemulsion and (2) the preparation of PS encapsulation around Ag nanoparticles to form Ag/PS composite particles through emulsion polymerization of styrene in the present of Ag nanoparticle.

As no additional passivator was added in microemulsion, the system could be considered as the stabilizer according to the XPS and UV-vis absorption spectra. The possible structures of Ag nanoparticles in microemulsion and emulsion systems are illustrated in Figure 8. The SDS molecules adsorbed on the silver nanoparticles might form surface ion pairs with  $\text{H}^+$  attached to the Ag surfaces, and the anionic surfactant SDS headgroups surrounded the  $\text{H}^+$  layer by electrostatic interactions. Thus, the hydrophobic SDSs tail chains would point outward, which enhanced the stability of Ag nanoparticles in styrene. The proposed scheme is experimentally supported by the studies on TOAB-capped gold nanopar-

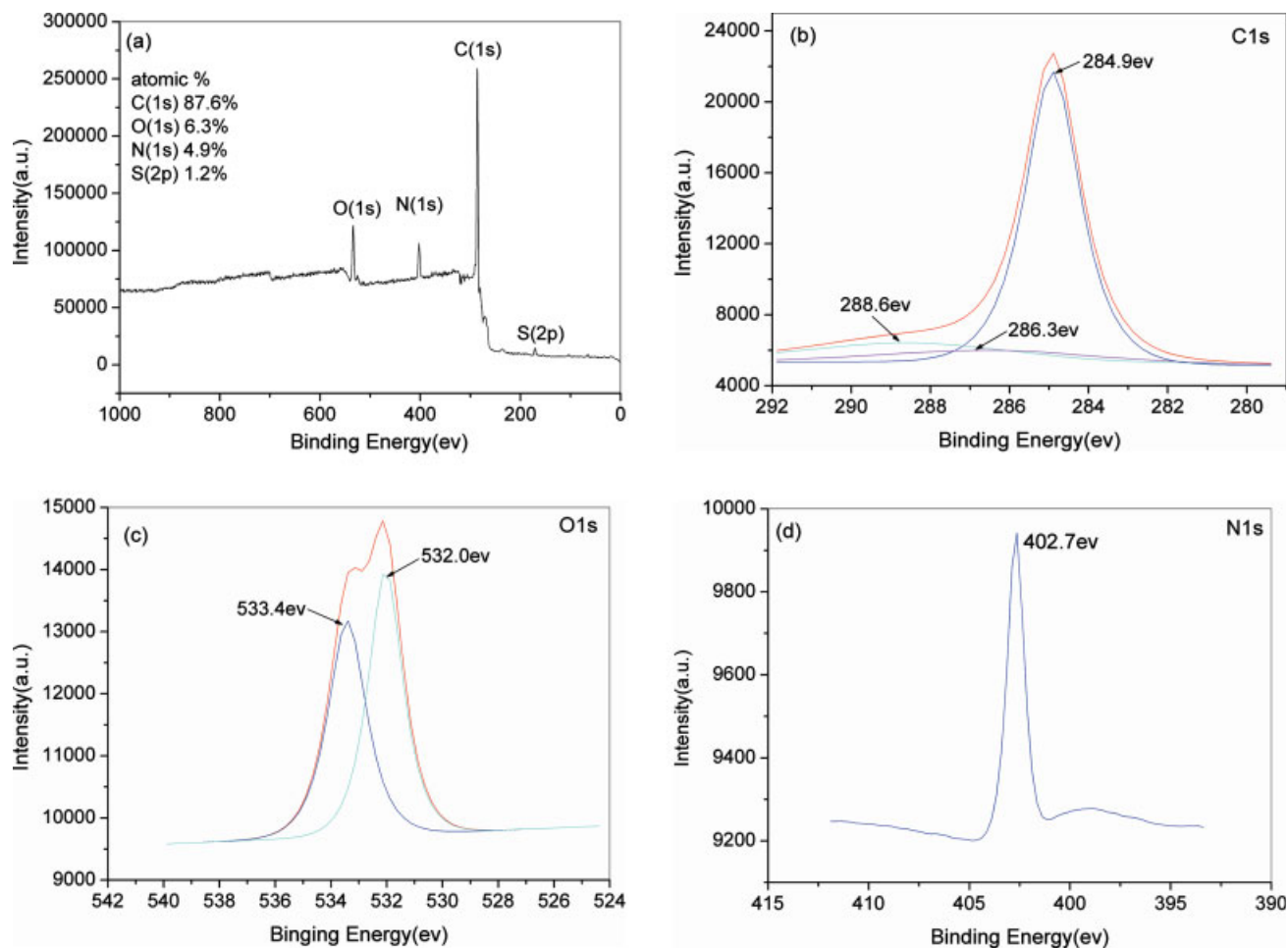
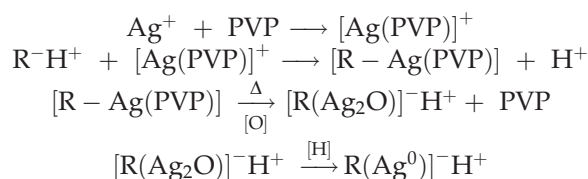


**Figure 7** Survey X-ray photoelectron spectra of Ag/PS nanocomposite particles. [Color figure can be viewed in the online issue, which is available at [www.interscience.wiley.com](http://www.interscience.wiley.com).]

ticles.<sup>28</sup> As the surfactant has two headgroups, which leads to a stronger interaction with Ag nanoparticles, the remained tail chains form a steric hindrance around the Ag nanoparticles, therefore the microemulsion system can protect the Ag nanoparticles from aggregation and act as a better stabilizer when comparing with other aqueous systems. As the microemulsion in the presence of Ag nanoparticles was used directly to be the monomer of emulsion polymerization for styrene, the aggregation of Ag nanoparticles in the reaction media could be broken down and the Ag nanoparticles can disperse well in styrene. With much monomer surrounding the surface of Ag nanoparticles through the attached surfactant were initiated, the primary composite particles continued to seize more monomer and initiator, and increased the molecular length until forming sphere particles with nanosize. In the whole process, PVP molecules surrounding Ag nanoparticles can separate the nanoparticles one by one and become the joining between Ag nanoparticles and polystyrene chains in the process of emulsion polymerization.

Therefore, the obtained encapsulation of Ag nanoparticles by polystyrene is uniform and Ag nanoparticles disperse well in nanocomposites. The mechanistic illustration of the earlier process is given later.



## CONCLUSIONS

Uniform Ag nanoparticles have been successfully prepared in reverse microemulsion and, at the same time, encapsulation of Ag nanoparticles by polystyrene had been achieved by emulsion polymerization. The reverse microemulsion with styrene as oil phase displayed excellent properties in the preparation and stabilization of Ag nanoparticles. These particles were characterized with SEM. The size distribution of the obtained Ag nanoparticles is narrow and the



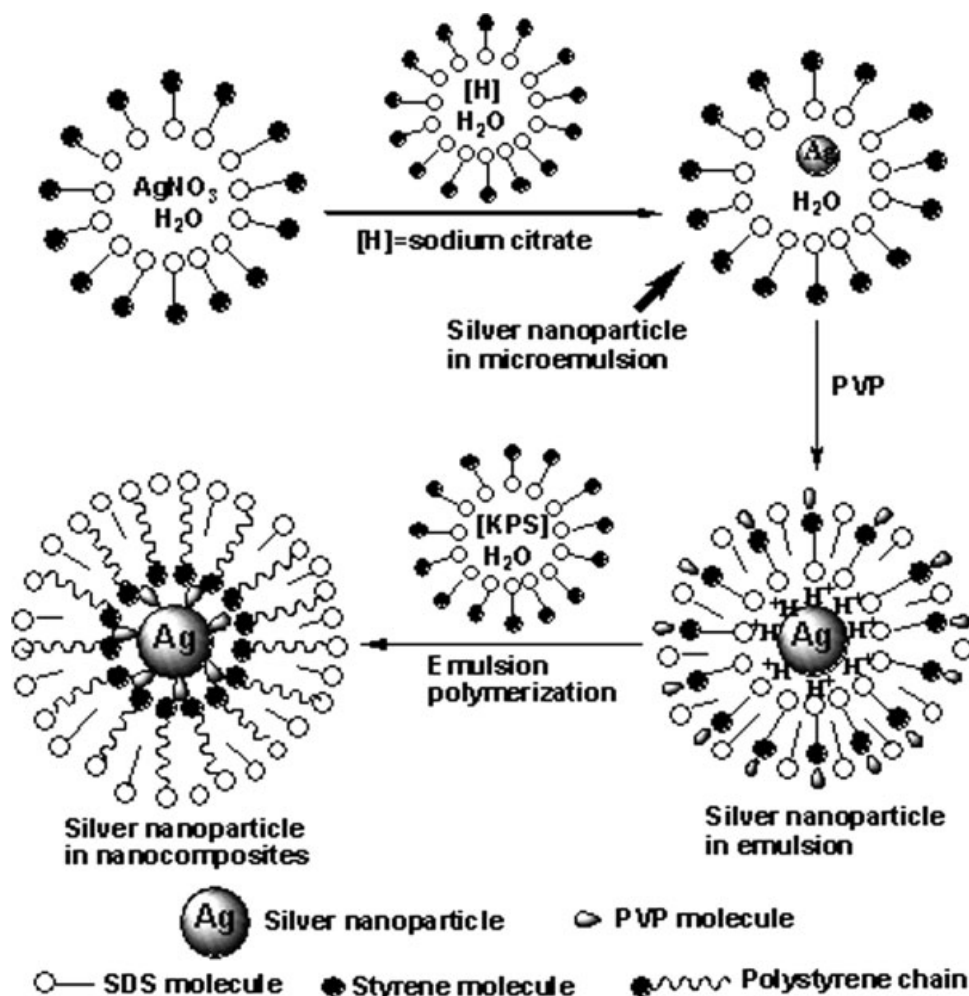


Figure 8 Schematic synthesis of Ag/PS nanoparticle.

surface of the polystyrene particles obtained in the presence of Ag nanoparticles was smooth and no silver bead was detected on the whole surface of the samples. On the other hands, the FTIR, XRD, XPS, and UV-vis spectroscopies of the Ag/PS composite particles provided another supporting evidence for the polystyrene-encapsulated silver nanoparticles structure. This technique could be extended to the preparation of a variety of metal nanoparticles under appropriate conditions.

The authors express sincere thanks to Applied Chemistry Emphases Laboratory of Hebei province for the helpful experiment supports.

## References

1. Temgire, M. K.; Joshi, S. S. *Radiat Phys Chem* 2004, 71, 1039.
2. Zhang W. Z.; Qiao X. L.; Chen J. G. *J Colloid Interface Sci* 2006, 302, 370.
3. Ledo, A.; Martinez, F.; Lopez-Quintela, M. A.; Rivas, J. *Phys B* 2007, 398, 273.
4. Mbhele, Z. M.; Sakmane, M. G.; Sittert, C. G. C. E.; Nedeljkovic, J. M.; Djokovic, V.; Luyt, A. S. *Chem Mater* 2003, 15, 5019.
5. Liang, G. D.; Bao, S. P.; Tjong, S. C. *Mater Sci Eng B* 2007, 142, 55.
6. Zhang, Z.; Han, M. *J Mater Chem Commun* 2003, 13, 641.
7. Mullick, K.; Witcomb, M. J.; Scurrall, M. S. *J Mater Sci* 2004, 39, 4459.
8. Firth, A. V.; Haggata, S. W.; Khanna, P. K.; Williams, S. J.; Allen, J. W.; Magennis, S. W.; Samuel, I. D. W.; Hamilton, D. J. *J Lumin* 2004, 109, 163.
9. Chandra, A.; Turng, L. S.; Gong, S. Q.; Hall, D. C.; Caulfield, D. F.; Yang, H. *Polym Compos* 2007, 28, 241.
10. Singh, N.; Khanna, P. K. *Mater Chem Phys* 2007, 104, 367.
11. Slistan, G. A.; Herrera, U. R.; Rivas, S. J. F.; Avalos, B. M.; Castellon, B. F. F.; Posada, A. A. *Phys E* 2005, 25, 438.
12. Yong, W. K.; Do Kyoung, L.; Kyung, J. L.; Byoung, R. M.; Jong, H. K. *J Polym Sci Part B: Polym Phys* 2007, 11, 1283.
13. Zhao, C. J.; Zhao, Q. T.; Zhao, Q. Z. *J Photochem Photobiol A* 2007, 187, 146.
14. Stepanov, A. L.; Popok, V. N.; Khaibullin, I. B.; Kreibig, U. *Nucl Instrum Methods Phys Res B* 2002, 191, 473.
15. Sowmitri, T.; Neha, K.; Noureddine, A.; Eric, H.; Joe, F.; Lenore, L. D. *J Appl Polym Sci* 2006, 5, 2938.
16. Stephan, T. D.; Panittamat, K.; Pranut, P. *Colloids Surf A* 2006, 289, 105.



17. Setua, P.; Chakraborty, A.; Seth, D. *Phys Chem C* 2007, 111, 3901.
18. Khanna, P. K.; Singh, N.; Charan, S.; Viswanath, A. K. *Mater Chem Phys* 2005, 92, 214.
19. Yilmazer, U.; Ozden, G. *Polym Compos* 2006, 27, 249.
20. Wu, D. Z.; Ge, X. W.; Huang, Y. H.; Zhang, Z. C.; Ye, Q. *Mater Lett* 2003, 57, 3549.
21. Nath, S.; Ghosh, S. K.; Kundu, S. *Mater Lett* 2005, 59, 3986.
22. Liu, W. J.; Zhang, Z. C.; He, W. D. *J Solid State Chem* 2006, 179, 1253.
23. Zhang, K.; Fu, Q.; Fan, J. H.; Zhou, D. H. *Mater Lett* 2005, 59, 3682.
24. Xu, J.; Han, X.; Liu, H. L.; Hu, Y.; *Colloids Surf A* 2006, 273, 179.
25. Petit, C.; Lixon, P.; Pileni, M. P. *J Phys Chem* 1993, 97, 12974.
26. Zhang, Z. Q.; Patel, R. C.; Kothari, R.; Johnson, C. P.; Friberg, S. E.; Aikens, P. A. *J Phys Chem B* 2000, 104, 1176.
27. He, S. T.; Yao, J. N.; Jiang, P.; Shi, D. X.; Zhang, H. X.; Xie, S. S.; Pang, S. J.; Gao, H. J. *Langmuir* 2001, 17, 1571.
28. Cheng, W.; Dong, S.; Wang, E. *Langmuir* 2003, 19, 9434.